Intermittency in dynamics of two-dimensional vortexlike defects

V. V. Lebedev*
Department of Physics of Complex Systems, Weizmann Institute of Science, Rehovot 76100, Israel
and Landau Institute for Theoretical Physics, RAS, Kosygina 2, Moscow 117940, Russia
(Received 15 July 1999; revised manuscript received 14 February 2000)

We examine high-order dynamical correlations of defects (vortices, disclinations, etc.) in thin films starting from the Langevin equation for the defect motion. We demonstrate that dynamical correlation functions F_{2n} of vorticity and disclinicity behave as $F_{2n}\sim y^2/r^{4n}$, where r is the characteristic scale and y is the renormalized fugacity. As a consequence, below the Berezinskii-Kosterlitz-Thouless transition temperature F_{2n} are characterized by anomalous scaling exponents. The behavior strongly differs from the normal law $F_{2n}\sim F_2^n$ occurring for simultaneous correlation functions, the nonsimultaneous correlation functions appear to be much larger. The phenomenon resembles intermittency in turbulence.

PACS number(s): 68.60.−p, 05.20.−y, 05.40.−a, 64.60.Ht

INTRODUCTION

It is well known that defects like quantum vortices, spin vortices, dislocations and disclinations play an essential role in the physics of low-temperature phases of thin films. Berezinskii [1] and then Kosterlitz and Thouless [2] recognized that there is a class of phase transitions in two-dimensional (2D) systems related to the defects. The main idea of their approach is that in 2D the defects can be treated as point objects interacting like charged particles. It is usually called Coulomb gas analogy. The low-temperature phase corresponds to a fluid constituted of bound uncharged defect-antidefect pairs, which is an insulator, whereas the high-temperature phase contains free charged particles and can be treated as plasma. Correspondingly, in the low-temperature phase the correlation length is infinite whereas in the high-temperature phase it is finite. A huge number of works are devoted to different aspects of the problem, see, e.g., the surveys [3–7]. The scheme proposed by Kosterlitz and Thouless can be applied to superfluid and hexatic films and planar 2D magnetics. It admits a generalization for crystalline films, see Refs. [8] and [9]. There are also applications to superconductive materials, especially to high-T_c superconductors, see, e.g., Ref. [10].

The dynamics of the films in the presence of the defects was considered in the papers in Refs. [11] and [12]. In the papers, a complete set of equations is formulated describing both motion of the defects and hydrodynamic degrees of freedom. Then, to obtain macroscopic dynamic equations, an averaging over an intermediate scale was performed. At the procedure the ''current density'' related to the defects was substituted by an expression proportional to the average ''electric field'' and to gradients of the temperature and of the chemical potential. The resulting equations perfectly correspond to the problems solved in the papers in Refs. [11] and [12]. Unfortunately, at the procedure, information concerning high-order correlations of the defect motion is lost. That is the motivation for the present paper where these high-order correlations are examined.

We start from the same ''microscopical'' equations of the defect dynamics as was accepted in Ref. [11]. Following the papers, we focus mainly on the case when the motion of the defects is determined by the Langevin equation describing an interplay between the Coulomb interaction and the thermal noise. We believe that the approach is correct for hexatic films (membranes, Langmuir films, freely suspended films). The situation is a bit more complicated for the vortices in superfluid films because of the Magnus force. Nevertheless, the equation for the vortices is close to the Langevin equation, see Ref. [11]. Similar equations can be formulated for the dislocations in crystalline films, see Ref. [12], for the vortices in superconductors in some interval of scales, see, e.g., Ref. [10], and for the spin vortices in planar 2D magnetics. We will not consider the last cases here, though our scheme is, generally, applicable to the systems. Treating nonsimultaneous correlation functions related to the defects, one should take into account creation and annihilation processes also. For this purpose we use the Doi technique [13] who demonstrated that dynamics of classical particles involved into chemical reactions can be examined in terms of the creation and annihilation operators, like in the quantum-field-theory.

We consider correlation functions F_{2n} of the ''charge density'' ρ (vorticity, disclinicity, etc.) provided that the so-called renormalized fugacity y is small. The inequality $y \ll 1$ is satisfied for large scales in the low-temperature phase and probably in some region of scales above T_c. In statics, the normal estimate $F_{2n}\sim F_2^n$ is valid at the condition. Surprisingly, the nonsimultaneous high-order correlation functions F_{2n} appear to be much larger than their normal estimate F_2^n. In the low-temperature phase the phenomenon reveals an anomalous scaling on large scales. The reason for such unusual behavior is that the main contribution to high-order nonsimultaneous correlation functions is associated with rare single defect-antidefect pairs. The situation resembles the intermittency phenomenon in turbulence, see, e.g., Ref. [14]. It can also be compared with nontrivial tails of probability distribution functions in the physics of disordered materials, see, e.g., Refs. [15] and [16]. Some preliminary results were published in Ref. [17].

*Electronic addresses: lwlebede@wicc.weizmann.ac.il and lebede@landau.ac.ru

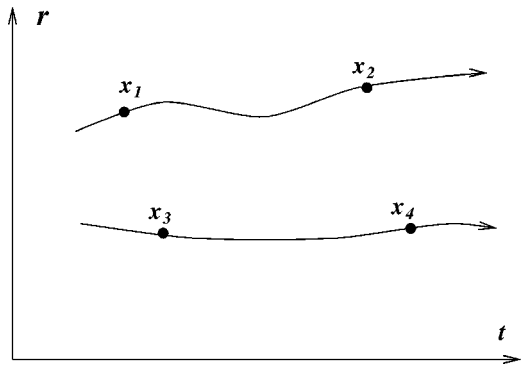

FIG. 1. Trajectories passing through given points.

Let us give a qualitative explanation of the phenomenon. To obtain a nonzero contribution to the correlation function $F_{2n}(t_1,\ldots,t_n;\boldsymbol{r}_1,\ldots,\boldsymbol{r}_n)$ one must consider trajectories of the particles passing through the points $\boldsymbol{r}_1,\ldots,\boldsymbol{r}_n$ at the time moments $t_1,\ldots,t_n$. The situation is illustrated in Fig. 1. The ''single-pair'' contribution has to be compared with a ''normal'' contribution associated with a number of defect-antidefect pairs. Though the normal contribution contains an additional large entropy factor it has also an additional small factor related to a small probability to observe a defect-antidefect pair with a separation larger than the core radius. As a result of the competition, the normal contribution appears to be smaller. To avoid a misunderstanding, let us stress that the arguments do not work for the simultaneous correlation functions. The reason is that trajectories of two defects cannot pass through $n>2$ points simultaneously, see Fig. 2. This mechanism of intermittency looks quite universal. It should be realized for any system of point objects correlated due to strong interaction.

Our paper is organized as follows. In Sec. I we remind some basic facts concerning static properties of the 2D defects and their dynamics and then we shortly review the Doi technique [13] suitable for our problem. In Sec. II we develop a diagrammatic representation for dynamical objects and examine the two-particle conditional probability that is extensively exploited in the subsequent consideration. In Sec. III we demonstrate how renormalization of different parameters can be obtained in the framework of our dynamic approach. Actually, the renormalization is reduced to the well-known static renormalization group equations. In Sec. IV we consider correlation functions of the ''charge density'' and ground the properties announced above. In Sec. V we generalize our procedure for the case of superfluid films. In Sec. VI we discuss the main results of our work and their possible relations to other systems. The extended version of the paper can be found in Ref. [18].

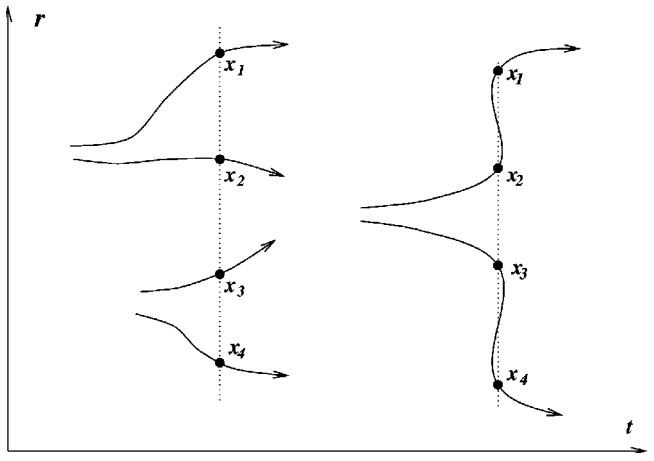

FIG. 2. Possible and impossible trajectories passing through four points at a given time moment.

I. BASIC RELATIONS

Static properties of the system of the vortexlike defects in thin films can be described quite universally. The starting point of the description is the free energy associated with the defects

$$\mathcal{F}=-\sum_{i\neq j} T\beta\, n_i n_j \ln\left(\frac{|\boldsymbol{x}_i-\boldsymbol{x}_j|}{a}\right)+\sum_j \mu(n_j), \qquad (1.1)$$

where the subscripts i,j label defects, $\boldsymbol{x}_i$ are positions of the defects, a is a cutoff parameter of the order of the size of the defect core, n_i are integer numbers determining the ''strength'' of the defects, β is a dimensionless T-dependent factor, and μ is the energy associated with the core. The expression (1.1) is correct for quantum vortices in superfluid films, for disclinations in hexatic films, and for spin vortices in 2D planar magnets. For dislocations in crystalline films the expression (1.1) has to be slightly modified [8], but the main peculiarity of the free energy, the logarithmic dependence on the separation, remains the same.

The Gibbs distribution $\exp(-\mathcal{F}/T)$ corresponding to the energy (1.1) can be treated as the partition function of two-dimensional point particles with charges n_j, with β playing a role of the ''inverse temperature.'' The parameter β can be considered also as the Coulomb coupling constant. Based on the electrostatic analogy, one can introduce the ''charge density''

$$\rho(\boldsymbol{r})=\sum_j n_j\delta(\boldsymbol{r}-\boldsymbol{x}_j). \qquad (1.2)$$

The quantity ρ is vorticity for superfluid films and disclinicity for hexatic films. We will treat the case where defects are produced by thermal fluctuations. Since both creation and annihilation processes conserve the ''charge'' we should accept that the total charge is zero:

$$\sum_j n_j=0.$$

It leads to the constraint

$$\int d^2r\,\rho(\boldsymbol{r})=0, \qquad (1.3)$$

where the integration is performed over the total area of the specimen.

Below we assume that for $|n|>1$ the core energy $\mu(n)$ is so large that such defects are hardly created. Then only defects with the charges $n_i=\pm 1$ should be taken into account.

We will call the objects with the charges $n_i=1$ defects and the objects with the charges $n_i=-1$ antidefects. Because of the constraint

$$\sum_j n_j=0$$

there can be simultaneously N defects and N antidefects in the system. Thus, the partition function of the system can be characterized via a set of probability distribution functions $\mathcal{P}_{2N}$ depending on coordinates of $2N$ ''particles.'' In accordance with Eq. (1.1) the functions can be written as

$$\mathcal{P}_{2N}(\boldsymbol{x}_1,\ldots,\boldsymbol{x}_{2N})=Z^{-1}\left(\frac{y_0}{a^2}\right)^{2N}\exp\left\{\sum_{i\neq j}\beta n_i n_j \ln\frac{|\boldsymbol{x}_i-\boldsymbol{x}_j|}{a}\right\}, \tag{1.4}$$

where Z is the sum over states and the quantity $y_0=\exp(-\mu/T)$ is usually called fugacity. The possibility to neglect charges with $|n|>1$ implies that the fugacity is small.

The low-temperature (insulator) phase can be treated as a system constituted of bound defect-antidefect pairs. In the high-temperature (plasma) phase there are unbound charges that essentially influence the system on scales larger than the correlation length r_c. We will treat the low-temperature phase and the region of scales between a and r_c in the high-temperature phase where one can neglect the role of the unbound charges and only the bound defect-antidefect pairs have to be taken into account. The presence of the pairs in the system leads to nontrivial ''dielectric'' properties of the medium. As a result, the interaction between the charges is modified, and the effect can be described in terms of a scale-dependent ''dielectric constant'' of the medium as is suggested in Ref. [2]. In other words, the effective coupling constant β becomes dependent on the separation between the charges.

The scale dependence of β can be described in the framework of the scheme proposed by Kosterlitz [19]. Namely, the partition function of the system can be integrated over separations of the defect-antidefect pairs between the core size a and a scale r. After the procedure that can be interpreted as shifting the core radius $a\to r$, the form of the probability distribution functions (1.4) is reproduced (with r instead of a), but the parameters β and y are renormalized. The r dependence of β and y is determined by the following renormalization-group equations found in Ref. [19]:

$$\frac{d\beta}{d\ln(r/a)}=-cy^2,\quad \frac{dy}{d\ln(r/a)}=(2-\beta)y, \tag{1.5}$$

where c is a numerical factor of order unity. The r-dependent function y is the renormalized fugacity. It determines a concentration of defects belonging to the bound pairs with separations of the order of r, the concentration can be estimated as y/r^2. The renormalized value of β determines the dependence of the strength of the Coulomb interaction on the separation between the charges. In the low-temperature phase, the effective value of β tends to a constant on large scales. The asymptotic value of β is larger than 2, the critical value $\beta=2$ corresponds to the transition temperature. In the asymptotic region, where β can be treated as r independent, the renormalized fugacity y remains r dependent. Its asymptotic behavior can easily be extracted from Eq. (1.5):

$$y\propto r^{2-\beta}. \tag{1.6}$$

Thus, in the low-temperature phase y tends to zero as the scale increases.

Let us turn to simultaneous correlation functions of the charge density ρ (1.2). The odd correlation functions are zero. Indeed, the system is symmetric under permuting defects and antidefects whereas the charge density (1.2) changes its sign at the permutation. The pair-correlation function can be written as (see, e.g., Ref. [20])

$$\langle\rho(\boldsymbol{r})\rho(0)\rangle\sim y^2(r)/r^4. \tag{1.7}$$

A generalization of the relation (1.7) can be obtained (see Ref. [21]) which is

$$\langle\rho(\boldsymbol{r}_1)\cdots\rho(\boldsymbol{r}_{2n})\rangle\sim\frac{y^{2n}(r_*)}{r_*^{4n}}\sim\langle\rho(\boldsymbol{r}_*)\rho(0)\rangle^n, \tag{1.8}$$

where all separations $|\boldsymbol{r}_i-\boldsymbol{r}_j|$ are assumed to be of the same order r_*. In the large-scale limit where β is saturated we have

$$\langle\rho(X\boldsymbol{r}_1)\cdots\rho(X\boldsymbol{r}_{2n})\rangle=X^{-2\beta n}\langle\rho(\boldsymbol{r}_1)\cdots\rho(\boldsymbol{r}_{2n})\rangle, \tag{1.9}$$

where X is an arbitrary factor. The relation (1.9) shows that the simultaneous statistics of ρ has normal scaling, that is scaling exponents of the correlation functions of the order $2n$ are equal to n times the scaling exponent of the pair-correlation function (1.7). We will demonstrate that the behavior of nonsimultaneous correlation functions of the charge density is quite different.

A. Dynamics

To examine dynamical characteristics of the system we should formulate a dynamical equation for a defect motion. Following Ref. [11] we accept the following stochastic equation

$$\frac{d\boldsymbol{x}_j}{dt}=-\frac{D}{T}\frac{\partial\mathcal{F}}{\partial\boldsymbol{x}_j}+\boldsymbol{\xi}_j, \tag{1.10}$$

determining the trajectory of the jth defect. Here $\mathcal{F}$ is the free energy (1.1), D is a diffusion coefficient, and $\boldsymbol{\xi}_j$ are Langevin forces with the correlation function

$$\langle\xi_{i,\alpha}(t_1)\xi_{j,\beta}(t_2)\rangle=2D\delta_{ij}\delta_{\alpha\beta}\delta(t_1-t_2). \tag{1.11}$$

The diffusion coefficient D determines mobility of the defects. We believe that the equation (1.10) is applicable to the dynamics of disclinations in hexatic films such as membranes, freely suspended films, and Langmuir films. The equation for the vortices in superfluid films is a bit more complicated. It is written in Sec. V where the correlation functions of the vorticity are analyzed.

The equations (1.10,1.11) describe trajectories of separate defects. We should also take into account annihilation and creation processes. Remember that we neglect defects with

$|n_j|>1$. Next, processes where a number of defect-antidefect pairs are created at the same point are suppressed since the probability of such events is small due to the energy associated with the cores of defects. Then we have to take into account the creation processes of single pairs solely, they are characterized by the creation rate $\overline{R}(r)$, which is a probability density for a defect-antidefect pair with the separation r to be created per unit time per unit area. The annihilation processes have to be characterized by the annihilation rate $R(r)$, which is a probability for a defect-antidefect pair to annihilate per unit time if the pair is separated by the distance r. Really, both $\overline{R}(r)$ and $R(r)$ are nonzero only if r is of the order of the core size a. Let us introduce the integrals

$$\overline{\lambda}=\int d^2r\,\overline{R}(r), \quad \lambda=\int d^2r\,R(r). \tag{1.12}$$

Here, the creation constant $\overline{\lambda}$ is a probability for a defect-antidefect pair to be created per unit time per unit area and λ is a constant having the same dimensionality as the diffusion coefficient D. Below, the diffusion coefficient D is put to unity by rescaling time. Then the annihilation constant λ is a dimensionless parameter of the order of unity and the creation constant $\overline{\lambda}$ can be estimated as

$$\overline{\lambda}\sim a^{-4}\exp(-2\mu/T), \tag{1.13}$$

which is the second power of the defect concentration.

The Gibbs distribution (1.4) must be a stationary solution of the master equations for the system. The condition imposes the following constraint on the creation and the annihilation rates:

$$\overline{R}(r)=\frac{y_0^2}{a^4}\left(\frac{a}{r}\right)^{2\beta}R(r), \tag{1.14}$$

where we imply $r>a$. The constraint (1.14) can be treated as the manifestation of the equilibrium state of the thermal bath, which in our case is related to short-scale fluctuations.

B. Quantum field formulation

The Doi technique [13] enables one to treat systems of classical particles where creation and annihilation processes occur. The main idea introduced by Doi is that correlation functions of different quantities characterizing the particles can be written in the form close to the one known in the quantum-field-theory. Of course there are some peculiarities related to the fact that for classical particles one should deal directly with probabilities whereas in the quantum-field-theory one starts from the scattering matrix. Nevertheless, the Doi technique enables, say, to formulate a diagrammatic expansion with the conventional rules. The technique was originally developed to describe systems of molecules involved in chemical reactions. But it is definitely applicable also to the system of point defects.

The Doi technique is formulated in terms of the creation $\hat{\psi}$ and annihilation ψ operators that satisfy the same commutation rules as the ones for Bose particles

$$[\psi(\boldsymbol{r}_1),\hat{\psi}(\boldsymbol{r}_2)]=\delta(\boldsymbol{r}_1-\boldsymbol{r}_2),$$

$$[\hat{\psi}(\boldsymbol{r}_1),\hat{\psi}(\boldsymbol{r}_2)]=[\psi(\boldsymbol{r}_1),\psi(\boldsymbol{r}_2)]=0. \tag{1.15}$$

For our system of defects we should introduce annihilation and creation operators $\psi_\pm$ and $\hat{\psi}_\pm$ where the subscripts $+$ and $-$ label fields related to the defects and to the antidefects. The state of the system at a time moment t can be written in terms of a ''quantum'' state

$$|t\rangle=\sum_{N=0}^{\infty}\frac{1}{(N!)^2}\int d^2x_1\cdots d^2x_N d^2z_1\cdots d^2z_N\mathcal{P}_{2N}\hat{\psi}_+(\boldsymbol{x}_1)\cdots\hat{\psi}_+(\boldsymbol{x}_N)\hat{\psi}_-(\boldsymbol{z}_1)\cdots\hat{\psi}_-(\boldsymbol{z}_N)|0\rangle, \tag{1.16}$$

where $\mathcal{P}_{2N}$ are the $2N$-particle probability densities and $|0\rangle$ designates the vacuum state: $\psi_\pm|0\rangle=0$. In accordance with the expression (1.16) an evolution of the quantum state $|t\rangle$ is determined by the master equations. The evolution equation can be written as

$$\partial_t|t\rangle=-\mathcal{H}|t\rangle, \tag{1.17}$$

where $\mathcal{H}$ is an operator expressed in terms of the fields $\psi_\pm$ and $\hat{\psi}_\pm$. By analogy with the quantum-field formulation it can be called the Hamiltonian operator or simply the Hamiltonian.

Quantities characterizing the system can be represented by corresponding operators, see Ref. [13]. Say, the operator of the charge density is

$$\tilde{\rho}=\hat{\psi}_+\psi_+-\hat{\psi}_-\psi_-. \tag{1.18}$$

If $\tilde{A}$ is such an operator corresponding to a quantity A, then an average value of the quantity at a time moment t can be expressed as

$$\langle A(t)\rangle=\langle 0|\exp\left[\int d^2r(\psi_++\psi_-)\right]\tilde{A}|t\rangle. \tag{1.19}$$

Correlation functions of different quantities can be presented analogously to Eq. (1.19). They can be rewritten as averages over an initial state if to introduce operators in the Heisenberg representation

$$\tilde{A}(t)=\exp[-(t_f-t)\mathcal{H}]\tilde{A}\exp[-(t-t_{in})\mathcal{H}]. \tag{1.20}$$

Then one can reformulate the problem of calculating correlation functions in terms of a functional integral, see Ref. [22]. Namely, we can write

$$\langle A_1(t_1)\dots A_n(t_n)\rangle = \int \mathcal{D}\hat{\psi}_\pm \mathcal{D}\psi_\pm \tilde{A}_1\dots\tilde{A}_n \times\exp\left\{-\int_{-\infty}^{t_f} dt\left[\mathcal{H}+\int d^2r(\hat{\psi}_+\partial_t\psi_+ + \hat{\psi}_-\partial_t\psi_-)\right] + \int d^2r[\psi_+(t_f,\boldsymbol{r})+\psi_-(t_f,\boldsymbol{r})]\right\}, \tag{1.21}$$

where $\psi_\pm, \hat{\psi}_\pm$ are to be interpreted as functions of t and $\boldsymbol{r}$. We assume that $t_f > t_1, \dots, t_n$ in Eq. (1.21). Deriving the expression one has taken the limit $t_{in}\to-\infty$ and assumed $|\text{in}\rangle = |0\rangle$. Because of the creation processes the vacuum has to be turned into a stationary state during the infinite time. To ensure convergence of the functional integral (1.21) the integration contour over the field $\hat{\psi}$ should go parallel to the imaginary axis.

II. DIAGRAMMATIC REPRESENTATION

Below, we apply the Doi technique to our particular problem. The explicit expression for the Hamiltonian determining the evolution of the defect system is

$$\mathcal{H} = \mathcal{H}_0 + \mathcal{H}_R + \mathcal{H}_\beta. \tag{2.1}$$

The explicit expressions for the terms entering Eq. (2.1) are

$$\mathcal{H}_0 = \int d^2r(\nabla\hat{\psi}_+\nabla\psi_+ + \nabla\hat{\psi}_-\nabla\psi_-) \tag{2.2}$$

$$\mathcal{H}_R = -\int d^2r_1\, d^2r_2[\overline{R}(\boldsymbol{r}_1-\boldsymbol{r}_2)(\hat{\psi}_{+,1}\hat{\psi}_{-,2}-1) + R(\boldsymbol{r}_1-\boldsymbol{r}_2)(\psi_{+,1}\psi_{-,2}-\hat{\psi}_{+,1}\hat{\psi}_{-,2}\psi_{+,1}\psi_{-,2})] \tag{2.3}$$

$$\mathcal{H}_\beta = 2\beta\int d^2r_1\, d^2r_2(\nabla\hat{\psi}_{+,1}\hat{\psi}_{-,2} - \hat{\psi}_{+,1}\nabla\hat{\psi}_{-,2}) \times\frac{\boldsymbol{r}_1-\boldsymbol{r}_2}{|\boldsymbol{r}_1-\boldsymbol{r}_2|^2}\psi_{+,1}\psi_{-,2} - 2\beta\int d^2r_1\, d^2r_2\left[\nabla\hat{\psi}_{+,1}\hat{\psi}_{+,2}\frac{\boldsymbol{r}_1-\boldsymbol{r}_2}{|\boldsymbol{r}_1-\boldsymbol{r}_2|^2}\psi_{+,1}\psi_{+,2} + \nabla\hat{\psi}_{-,1}\hat{\psi}_{-,2}\frac{\boldsymbol{r}_1-\boldsymbol{r}_2}{|\boldsymbol{r}_1-\boldsymbol{r}_2|^2}\psi_{-,1}\psi_{-,2}\right], \tag{2.4}$$

where $\psi_{+,1} = \psi_+(t,\boldsymbol{r}_1)$ and so further. The diffusive contribution (2.2) is related to the Langevin forces, in Eq. (2.3), where R is the annihilation rate and $\overline{R}$ is the creation rate for the defect-antidefect pairs (the quantities were introduced in Sec. I), and the term (2.4) describes the Coulomb interaction.

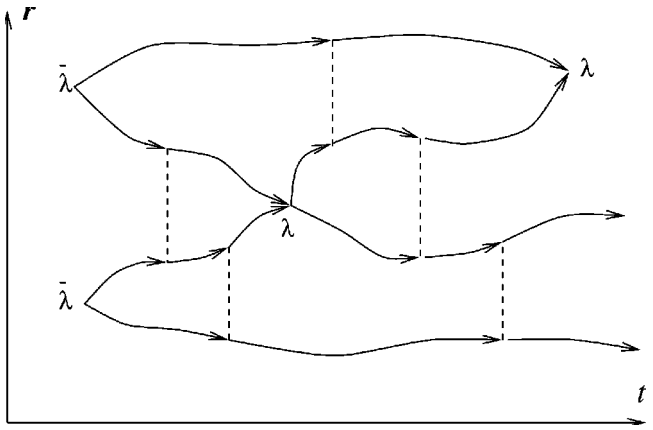

FIG. 3. Typical diagram block.

Substituting the expression (2.1) into Eq. (1.21) and expanding the exponent over $\mathcal{H}_R$ and $\mathcal{H}_\beta$ one can obtain a conventional perturbation series for calculating different correlation functions of $\psi, \hat{\psi}$. The series is an expansion over R, $\overline{R}$, and β in terms of the conventional diffusion propagators:

$$G(t,\boldsymbol{r}) = \langle\psi_+(t,\boldsymbol{r})\hat{\psi}_+(0,0)\rangle_0 = \langle\psi_-(t,\boldsymbol{r})\hat{\psi}_-(0,0)\rangle_0 = \frac{\theta(t)}{4\pi t}\exp\left(-\frac{r^2}{4t}\right), \tag{2.5}$$

where $\theta(t)$ is the step function. However, effects related to the Coulomb interaction and to the annihilation processes are not weak. Therefore one must take into account the Coulomb interaction and the annihilation processes exactly. In other words, when calculating the correlation functions, one must consider the complete series over β and R. Fortunately, the expansion over $\overline{R}$ is equivalent to an expansion over the fugacity y, which is assumed to be a small parameter. Therefore we can take only principal terms in the expansion over $\overline{R}$.

The perturbation expansion can be formulated as a diagrammatic series. We develop the diagrammatic technique starting from the representation (1.21), pushing the final time t_f to the far future. We depict the propagator (2.5) by a line directed from $\hat{\psi}$ to ψ. The term with the creation rate $\overline{R}$ in Eq. (2.1) generates vertices where two propagator lines start, the vertices correspond to the defect-antidefect creation processes. The Coulomb term in Eq. (2.1) generates two-point objects, which we will designate by dashed lines, which describes the Coulomb interaction of defects located in points connected by the line. And the term proportional to the annihilation rate R in Eq. (2.1) produces two types of vertices. First, it produces vortices where two propagator lines finish, that corresponds to an annihilation process. Second, it produces fourth-order vertices that correspond to an effective interaction related to a finite probability for a defect-antidefect pair to annihilate, see Ref. [13]. A typical diagram block is presented in Fig. 3. The block is drawn in real $\boldsymbol{r}-t$ space time. The curves constituted of the propagator lines can be interpreted as trajectories of defects and antidefects. Due to causality the particles always move forward in time. Note that the dashed lines corresponding to the Coulomb

interaction are perpendicular to the t axis since the interaction is simultaneous.

A. Pair conditional probability

In this subsection we examine an auxiliary object that will be needed at intermediate stages of subsequent calculations. The object is the following correlation function

$$M(t_2-t_1,\boldsymbol{r}_1,\boldsymbol{r}_2,\boldsymbol{r}_3,\boldsymbol{r}_4)$$

$$=\langle\psi_+(t_2,\boldsymbol{r}_1)\psi_-(t_2,\boldsymbol{r}_2)\hat{\psi}_+(t_1,\boldsymbol{r}_3)\hat{\psi}_-(t_1,\boldsymbol{r}_4)\rangle. \quad (2.6)$$

For a stationary case the average (2.6) depends on the difference $t=t_2-t_1$ only. Due to causality, M is equal to zero provided $t<0$. The quantity (2.6) can be interpreted as a probability density to find a defect and an antidefect at the time moment t_2 in the points $\boldsymbol{r}_1$ and $\boldsymbol{r}_2$ provided they were located in the points $\boldsymbol{r}_3$ and $\boldsymbol{r}_4$ at the time moment t_1. It can be considered also as a two-particle matrix element of the evolution operator $\exp[-(t_2-t_1)\mathcal{H}]$.

As we explained above, the perturbation series in terms of the creation rate $\overline{R}$ is an expansion over a small parameter, which is the fugacity. Here we examine the principal contribution to the conditional probability (2.6) which is of the zero order over $\overline{R}$. Then the average (2.6) can be represented as a series of diagrams of the type depicted in Fig. 4. One can interpret the picture as trajectories of a defect and of an antidefect that are driven by the Langevin forces, and are influenced the Coulomb interaction (dashed lines) and the effective interaction associated with the annihilation processes (point vertex). Note that in this approximation, direct annihilation events do not contribute to the conditional probability (2.6) since they would lead to terminating the lines in the diagrams.

It is of crucial importance that both the Coulomb interaction and the effective interaction associated with the annihilation processes are local in time. Therefore all the diagrams representing the conditional probability (2.6) are ladder diagrams, like in Fig. 4. Summing up the ladder sequence we get an equation for M that can be written in the differential form

$$\partial_t M=(\nabla_1^2+\nabla_2^2)M+2\beta(\nabla_1-\nabla_2)\left[\frac{\boldsymbol{r}_1-\boldsymbol{r}_2}{|\boldsymbol{r}_1-\boldsymbol{r}_2|^2}M\right]$$

$$-R(\boldsymbol{r}_1-\boldsymbol{r}_2)M+\delta(t)\,\delta(\boldsymbol{r}_1-\boldsymbol{r}_3)\,\delta(\boldsymbol{r}_2-\boldsymbol{r}_4). \quad (2.7)$$

Since $M=0$ at $t<0$ we conclude from Eq. (2.7) that at $t\to+0$,

$$M(t,\boldsymbol{r}_1,\boldsymbol{r}_2,\boldsymbol{r}_3,\boldsymbol{r}_4)\to\delta(\boldsymbol{r}_1-\boldsymbol{r}_3)\,\delta(\boldsymbol{r}_2-\boldsymbol{r}_4). \quad (2.8)$$

The solution of Eq. (2.7) can be written in a multiplicative form

$$M=\frac{1}{2\pi t}\exp\left\{-\frac{(2\varrho-\boldsymbol{r}_3-\boldsymbol{r}_4)^2}{8t}\right\}S(t,\boldsymbol{r},\boldsymbol{r}_0), \quad (2.9)$$

where the function S satisfies the following equation

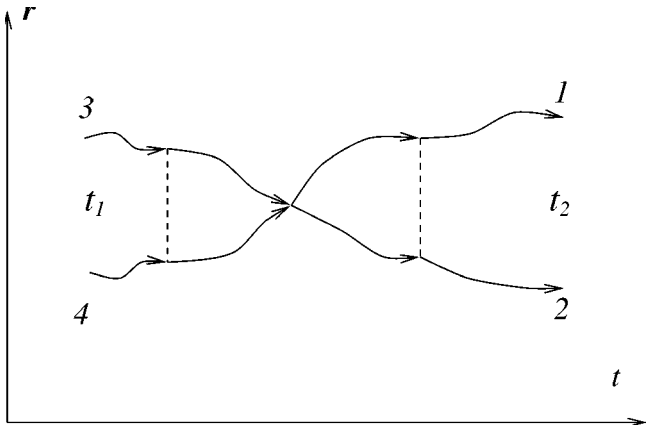

FIG. 4. Typical diagram for the conditional probability M.

$$\partial_t S=2\nabla^2 S+4\beta\nabla\left(\frac{\boldsymbol{r}}{r^2}S\right)-R(r)S+\delta(t)\,\delta(\boldsymbol{r}-\boldsymbol{r}_0). \quad (2.10)$$

Here

$$\boldsymbol{r}=\boldsymbol{r}_1-\boldsymbol{r}_2,\quad \varrho=\frac{\boldsymbol{r}_1+\boldsymbol{r}_2}{2},\quad \boldsymbol{r}_0=\boldsymbol{r}_3-\boldsymbol{r}_4. \quad (2.11)$$

In accordance with Eq. (2.9), a motion of the mass center and the relative motion of the defects are separated. The motion of the mass center is purely diffusive whereas the relative motion is strongly influenced by the interaction. The function S can be treated as the probability density for the relative motion of the defect-antidefect pair. It is natural to expand the function into the Fourier series over the angle φ between the vectors $\boldsymbol{r}$ and $\boldsymbol{r}_0$:

$$S(t,\boldsymbol{r},\boldsymbol{r}_0)=\sum_{-\infty}^{+\infty}S_m(t,r,r_0)\exp(im\varphi). \quad (2.12)$$

Motions corresponding to different angular harmonics are separated. In terms of the angular harmonics, Eq. (2.10) is rewritten as

$$\frac{1}{2}\partial_t S_m=\left[\partial_r^2+(1+2\beta)\frac{1}{r}\partial_r-\frac{m^2}{r^2}\right]S_m-\frac{1}{2}R(r)S_m$$

$$+\frac{1}{4\pi r_0}\delta(t)\,\delta(r-r_0). \quad (2.13)$$

It is possible to get equations for S analogous to Eqs. (2.10) and (2.13) in terms of $\boldsymbol{r}_0$. They have practically the same form as Eqs. (2.10) and (2.13). The only difference is in the sign of β, which is opposite. That leads to the relation

$$S_m(t,r,r_0)=\left(\frac{r_0}{r}\right)^{2\beta}S_m(t,r_0,r). \quad (2.14)$$

Let us stress that the relation (2.14) is correct for an arbitrary function $R(r)$.

Consider a behavior of the angular harmonics $S_m(t,r,r_0)$ at small r. More precisely, we assume $t\gg a^2$ and examine the region $\sqrt{t}\gg r\gg a$. Then it is possible to use Eq. (2.13) with the time derivative and the annihilation term neglected. As a result we get

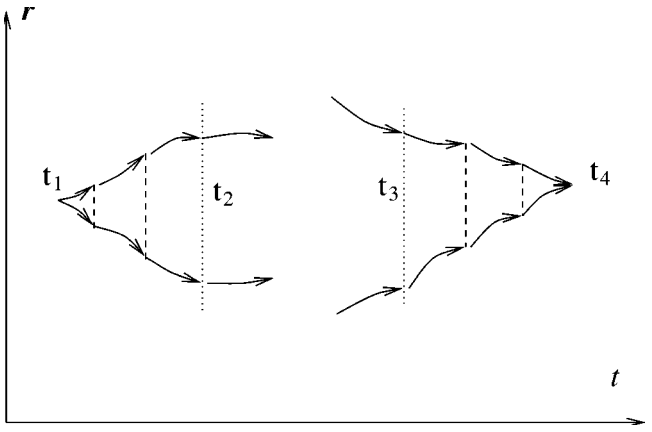

FIG. 5. Vicinities of creation and annihilation points.

$$S_m = C_{1,m} r^{\nu-\beta} + C_{2,m} r^{\nu-\beta} (r/a)^{-2\nu}, \tag{2.15}$$

$$\nu = \sqrt{\beta^2 + m^2}, \tag{2.16}$$

where $C_{1,m}, C_{2,m}$ are some factors dependent on t and r_0. The ratio of the factors is determined by a concrete r dependence of the annihilation rate R; one can assert only that C_{1m} and C_{2m} are of the same order. Therefore, if we consider the behavior of the function S for $r \gg a$, then the second term on the right-hand side of Eq. (2.15) can be neglected. In other words, being interested in the scales $r \gg a$, we can solve Eq. (2.13) neglecting the annihilation term and requiring a finite value of S_m at $r \to 0$ instead. The requirement can be treated as the boundary condition for S_m at small r. The other boundary condition is that S_m tends to zero at $r \to \infty$. Then

$$S_m = \frac{1}{8\pi t} \left(\frac{r_0}{r} \right)^{\beta} \exp\left(-\frac{r^2 + r_0^2}{8t} \right) I_\nu \left(\frac{r r_0}{4t} \right), \tag{2.17}$$

where I is the modified Bessel function and ν is introduced by Eq. (2.16).

Note that the Coulomb term in Eq. (2.10) produces a probability flux to the origin. To find it we should integrate Eq. (2.10) over a disk of a radius $a \ll r \ll \sqrt{t}$ centered at the origin and single out the contribution to $\partial_t \int d^2 r\, S$ associated with the Coulomb term. Then we find the flux $\lambda_r C_{1,0}$ where

$$\lambda_r = 8\pi\beta. \tag{2.18}$$

One can treat the quantity (2.18) as the renormalized (''dressed'') value of the annihilation constant. Now we understand why the solution (2.17) (realized at $r \gg a$) is insensitive to a particular form of the annihilation rate. The probability for a defect-antidefect pair with the separation $r \gg a$ to annihilate is determined by the Coulomb attraction. And only the behavior of the probability density at $r \sim a$ is sensitive to the particular form of the annihilation rate $R(r)$: The coefficients $C_{2,m}$ in Eq. (2.15) are positive if $\lambda < \lambda_r$ and are negative if $\lambda > \lambda_r$.

III. RENORMALIZATION

In this section we are going to discuss effects related to high-order terms over the creation rate $\overline{R}$. The effects are relevant only near the transition point where β is close to 2. Then the influence of small-scale defect-antidefect pairs on larger scales becomes essential. In the situation the most natural language is the renormalization-group approach. One can formulate a renormalization-group procedure in the spirit of Kosterlitz, Ref. [19]. We will single out blocks corresponding to small separations of the pairs and treat them as renormalized quantities entering the Hamiltonian (2.1).

A. Creation and annihilation rates

Sizes of the pairs are small near creation and near annihilation points. Here, we consider vicinities of the points. Then it is possible to neglect the interaction of the defect and of the antidefect with the environment. Thus we turn to the situation when only a single pair can be treated. If this is the case, then one should analyze diagram blocks of the type drawn in Fig. 5. The left part of the figure corresponds to a vicinity of the creation occurring at a time moment t_1 and the right part of the figure corresponds to a vicinity of the annihilation occurring at a time moment t_4.

Now we consider processes occurring during a time interval τ from the creation time t_1. One can separately treat a block corresponding to the time interval from t_1 until $t_2 = t_1 + \tau$. For this purpose we use the well-known property of the propagators (2.5):

$$G(s_3 - s_1, \boldsymbol{r}) = \int d^2x\, G(s_3 - s_2, \boldsymbol{r} - \boldsymbol{x}) G(s_2 - s_1, \boldsymbol{x}), \tag{3.1}$$

where $s_3 > s_2 > s_1$. For each diagram we extract propagators G containing t_2 inside their time interval and represent the propagators such as in Eq. (3.1) believing $s_2 = t_2$. The procedure is reflected in Fig. 5 where the dotted line represents a plane $t = t_2$ in the $\boldsymbol{r} - t$ space time and the integration in Eq. (3.1) corresponds to the integration in the plane. As a result, the block to the left of the plane is separated, it is characterized by the time separation τ and by two points $\boldsymbol{r}_1$ and $\boldsymbol{r}_2$ lying in the plane, the points are intersections of the plane with the trajectories of the particles. The block has to be inserted into more complicated objects via a convolution over $\boldsymbol{r}_1$ and $\boldsymbol{r}_2$.

The same is true for the vicinity of the annihilation point also. Let us take a time moment t_3 separated by a time interval $\tau \gg a^2$ from an annihilation time t_4. Then it is possible to introduce the block that is a sum of the diagrams where the trajectories of the annihilating particles start from two given points $\boldsymbol{r}_3$ and $\boldsymbol{r}_4$ at $t = t_3$. The block has to be inserted into more complicated objects via a convolution over the points. In the vicinity of the annihilation point we can take into account the interaction of the annihilating defect-antidefect pair solely. That leads to the same ladder diagrams treated in Sec. II. Therefore we can write an expression for the block without an additional analysis

$$R_\tau(r_0) = \int d^2 r_1\, d^2 r_2\, R(\boldsymbol{r}) M(\tau, \boldsymbol{r}_1, \boldsymbol{r}_2, \boldsymbol{r}_3, \boldsymbol{r}_4)$$

$$= \int d^2 r\, S(\tau, \boldsymbol{r}, \boldsymbol{r}_0) R(r). \tag{3.2}$$

Here $\boldsymbol{r}$ and $\boldsymbol{r}_0$ are defined by Eq. (2.11), M is the conditional probability (2.6), S is the conditional probability for the rela-

tive motion of the defects, see Eq. (2.9), it is the solution of Eq. (2.10). The physical meaning of the quantity $R_\tau(r_0)$ is a distribution of the annihilating particles over the separation r_0 between the particles at the time moment t_3. It is natural to name this distribution the ''dressed'' annihilation rate since the quantity determines a probability for the particles to annihilate after the time interval τ. Note that all processes occurring on scales larger than $\sqrt{\tau}$ are sensitive only to this dressed quantity.

Let us substitute into Eq. (3.2) the product RS expressed from Eq. (2.10). The terms with the total derivatives give zero contribution to the integral over $\boldsymbol{r}$ and we get

$$R_\tau(r_0) = -\partial_\tau \int d^2r\, S(\tau,\boldsymbol{r},\boldsymbol{r}_0). \tag{3.3}$$

Since $S(\tau)$ tends to zero at $\tau\to+\infty$ and is zero for negative τ, we get from Eq. (3.3),

$$\int d\tau R_\tau(r_0) = 1. \tag{3.4}$$

The relation means that the total probability of a given pair to annihilate is equal to unity. As is seen from Eq. (2.15) at the condition $\tau \gg a^2$, the main contribution to the integral on the right-hand side of Eq. (3.3) is associated with the region $r\sim\sqrt{\tau}$ and therefore the contribution to the integral associated with the region $r\sim a$ is negligible. Therefore, we can use the expression (2.12) with Eq. (2.17). Substituting it into Eq. (3.3), we get a universal expression for the dressed quantity $R_\tau(r_0)$, which is insensitive to the bare quantity $R(r)$.

In Sec. II we established the renormalized value (2.18) of the annihilation constant λ. This analysis concerned the fourth-order interaction term written in Eq. (2.1). Below we demonstrate that the renormalized coefficient of the second-order annihilation term has the same value, independent of the bare one. In accordance with Eq. (1.12), to find the renormalized value λ_r we should calculate the integral of $R_\tau(r_0)$. At $\tau \gg a^2$, the value of the integral is independent of τ and coincides with the value written in Eq. (2.18), as one anticipated:

$$\lambda_r = \int d^2r_0\, R_\tau(r_0) = 8\pi\beta. \tag{3.5}$$

The phenomenon resembles the renormalization of the reaction rate due to diffusion, see Refs. [13] and [23].

Analogously, one can introduce the renormalized creation rate $\overline{R}_\tau(r)$, which is determined by the block describing the vicinity of the creation point (see Fig. 5). Summing up the same ladder sequence of the diagrams we get

$$\overline{R}_\tau(\boldsymbol{r}) = \int d^2r_3\, d^2r_4\, \overline{R}(\boldsymbol{r}_0) M(\tau,\boldsymbol{r}_1,\boldsymbol{r}_2,\boldsymbol{r}_3,\boldsymbol{r}_4)$$

$$= \int d^2r_0\, \overline{R}(\boldsymbol{r}_0) S(\tau,\boldsymbol{r},\boldsymbol{r}_0). \tag{3.6}$$

Here $\boldsymbol{r}$ and $\boldsymbol{r}_0$ are defined by Eq. (2.11), and M is the conditional probability (2.6), S is the conditional probability for the relative motion of the defects, see Eq. (2.9). Using the relations (1.14) and (2.14) we get from Eq. (3.6),

$$\overline{R}_\tau(\boldsymbol{r}) = \frac{y_0^2}{a^4}\left(\frac{a}{r}\right)^{2\beta} R_\tau(r). \tag{3.7}$$

Thus we see that the relation (1.14) is reproduced for the renormalized quantities R_τ and $\overline{R}_\tau$.

The renormalized creation rate $\overline{R}_\tau(\boldsymbol{r})$ can be interpreted as a probability density to find a defect-antidefect pair with a space separation $\boldsymbol{r}$ provided the pair was born on time separated by τ from the measurement. Let us calculate the total probability density $\overline{\lambda}_r$ to find the defect-antidefect pair at a fixed time separation τ regarding $\tau \gg a^2$. The probability is determined by the integral of $\overline{R}_\tau(\boldsymbol{r})$ over $\boldsymbol{r}$. We conclude from expressions (2.17) and (3.3) that the integral is determined by the region $r\sim\sqrt{\tau}$. Taking into account Eq. (3.5) we get

$$\overline{\lambda}_r = \int d^2r\, \overline{R}_\tau(\boldsymbol{r}) \sim \frac{y_0^2}{a^4}\left(\frac{a^2}{\tau}\right)^{\beta}. \tag{3.8}$$

We see that due to annihilation of defects at collisions the total probability diminishes when increasing the time separation τ as a power of τ. The property can be interpreted as follows: The majority of defect-antidefect pairs annihilate fast after their creation and only a minor part of the defects achieve a separation $r \gg a$. The probability of such an event is proportional to $(r/a)^{-2\beta}$.

The results obtained in this subsection are correct if the variation of the coupling constant β on the scale interval $a < r < \sqrt{\tau}$ is small. The existence of such an interval is justified by the assumed small value of the fugacity y_0. Near T_c variations of β on a wide region of scales can be relevant. Then the consideration needs a generalization made in the last subsection of this section.

B. Coulomb interaction and diffusion coefficient

Let us consider the renormalization of the Coulomb interaction related to small defect-antidefect pairs. It is known that the influence of such pairs can be described in terms of a contribution to the effective dielectric constant, see Ref. [2]. The picture is naturally generalized for the dynamics.

A typical diagram contributing to renormalization of the effective ''dielectric constant'' is drawn in Fig. 6. There we see a loop composed of the trajectories of a defect and of an antidefect that annihilate after their creation. There are also two ''external'' dashed lines corresponding to the interaction of the defect-antidefect pair with an environment. Besides the diagrams of the type drawn in Fig. 6, there are also diagrams with two external dashed lines attached to the same trajectory. We draw the external lines with arrows to remember that two sides of the dashed line are not equivalent.

As previously, we can dissect the diagram into parts that can be treated separately. Then the answer can be found as a convolution of the corresponding expressions. We perform the dissection along the planes in the $\boldsymbol{r}-t$ space time perpendicular to the t axis and corresponding to the time moments t_2 and t_3 of the external Coulomb lines. In Fig. 6 the dissection is shown by the dotted lines. We see that the loop is divided into three parts.

The left part of the loop implying the integration over the time t_1 (see Fig. 6) corresponds to

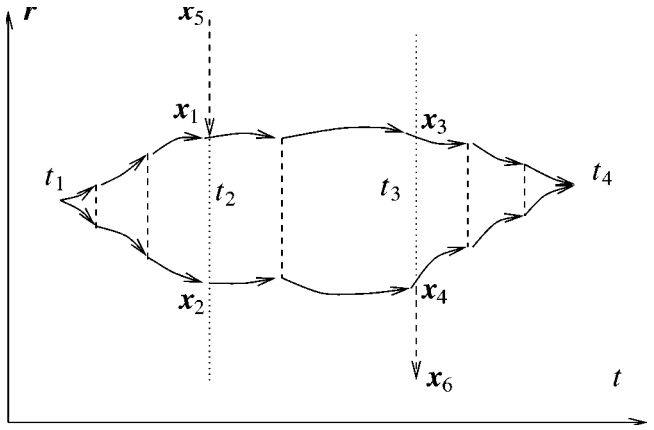

FIG. 6. Typical diagram contributing to renormalization of the effective dielectric constant.

$$\int_0^\infty d\tau \int d^2r_3\, d^2r_4\, \overline{R}(\boldsymbol{r}_3-\boldsymbol{r}_4) M(\tau,\boldsymbol{x}_1,\boldsymbol{x}_2,\boldsymbol{r}_3,\boldsymbol{r}_4) = \int_0^\infty d\tau\, \overline{R}_\tau(|\boldsymbol{x}_1-\boldsymbol{x}_2|). \tag{3.9}$$

Substituting here Eq. (3.7) and using Eq. (3.4) we get

$$\int_0^\infty d\tau\, \overline{R}_\tau(r) = \frac{y_0^2}{a^4}\left(\frac{a}{r}\right)^{2\beta}. \tag{3.10}$$

The central part of the diagram depicted in Fig. 6 corresponds to the conditional probability (2.6) $M(t_3-t_2,\boldsymbol{x}_3,\boldsymbol{x}_4,\boldsymbol{x}_1,\boldsymbol{x}_2)$. And the right part of the diagram in Fig. 6 corresponds to the integral (3.4). The relation can be recognized as a manifestation of independence of all results of the final time t_f in the relation (1.21). If we chose $t_f=t_3$ then the right part of the diagram in Fig. 6 disappears and we should substitute one instead, in accordance with Eq. (3.4).

The structure of the diagram depicted in Fig. 6 shows that the block related to the defect-antidefect pair can be treated as a self-energy insertion to the line corresponding to the Coulomb interaction. Thus it is natural to expect that this insertion can be treated as a contribution to the ''dielectric constant,'' leading to a renormalization of the Coulomb constant β:

$$\Delta\beta \sim -y_0^2 \int \frac{dr}{r}\left(\frac{a}{r}\right)^{2\beta-4}. \tag{3.11}$$

The expression can be treated as an integral over the characteristic sizes of the defect-antidefect pairs.

One may try to find more complicated blocks contributing to a renormalization of the Coulomb coupling constant β. An example of such block is depicted in Fig. 7 where a number (three) ''external'' lines are attached to the loop corresponding to the trajectories of the defect-antidefect pair. One can easily check that the block depicted in Fig. 7 gives a correction to the Coulomb force that diminishes faster than r^{-1} at increasing the distance r between the interacting particles. Therefore the contribution is irrelevant. The same is true for more complicated diagrams of the same type.

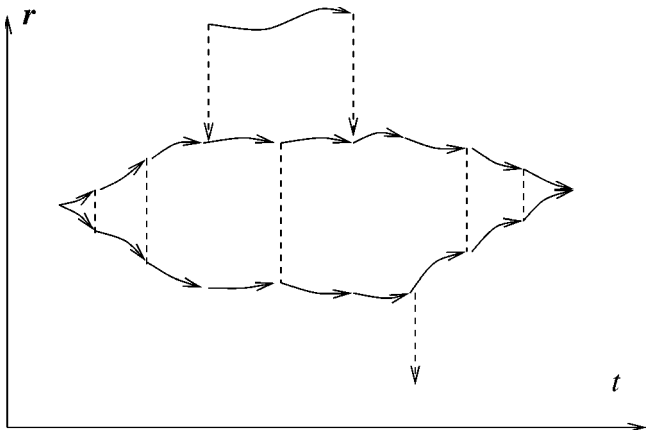

FIG. 7. A more complicated diagram giving a correction to the Coulomb interaction.

We can also consider blocks that can be treated as contributions to the diffusion coefficient D introduced by Eqs. (1.10) and (1.11). An example is depicted in Fig. 8, where the block between two dotted lines is a self-energy insertion to the propagator (2.5) which gives the renormalization of the diffusion coefficient. We will assume that the fields $\psi_\pm$ are corrected to keep the term (2.2) unchanged. Then the contribution (3.12) has to be extracted from the renormalization of the coefficient in front of the time derivatives.

To analyze the correction ΔD quantitatively one should know a three-particle conditional probability that is more complicated than the two-particle conditional probability (2.6). Fortunately, one can estimate the value of ΔD without detailed calculations. The point is that the dependence of ΔD on the cutoff a can be produced only by regions near the creation or near the annihilation point (which are designated by ovals in Fig. 8). The regions can be analyzed in terms of the two-particle conditional probability (2.6) since only the interaction of the nearest ''particles'' is relevant there. We already know the answer: the region near the creation point produces the renormalized creation rate (3.6) whereas the region near the annihilation point produce no a dependence. Then simple dimensional estimates give the answer similar to expression (3.11),

$$\Delta D \sim -y_0^2 \int \frac{dr}{r}\left(\frac{a}{r}\right)^{2\beta-4}. \tag{3.12}$$

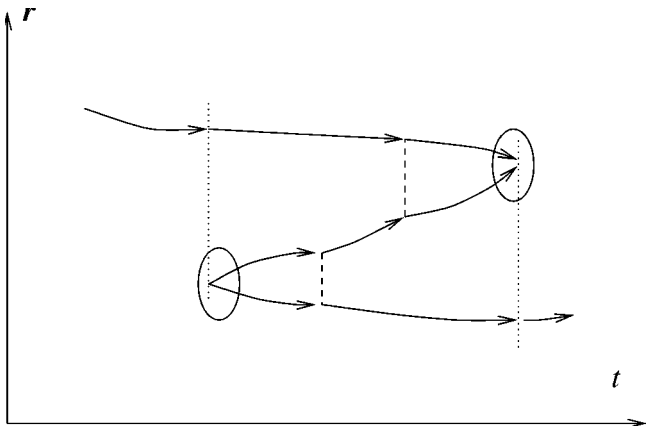

FIG. 8. Illustration to the renormalization of the diffusion coefficient.

Remember that the bare value of D is assumed to be equal to unity.

C. Summary

In the preceding subsection we obtained the expressions for the corrections (3.11) and (3.12) of the Coulomb constant and of the diffusion coefficient in the main order over the fugacity y_0. Now we are going to discuss high-order corrections over y_0, which in statics leads to the renormalization-group equations (1.5). It will be more convenient for us to proceed in spirit of the Kosterlitz renormalization-group scheme. Namely, we see that expressions (3.11) and (3.12) are written as integrals over the space variable r, which can be treated as the size of a defect-antidefect pair. We can first perform the integration over a restricted interval of the sizes, what gives slightly renormalized values of the coupling constants. Then we can repeat the integration. In the limit this multistep procedure gives the renormalization group equations for the coupling constants, as Kosterlitz suggested. On the diagrammatic language the procedure means that we gradually substitute blocks corresponding to small separations between the particles by their effective values relative to larger scales. The procedure can also be considered as increasing an effective size of the defects $a \to r$. Then the renormalization of the coupling constants can be described in terms of the differential renormalization-group equations.

At each step of the procedure we deal with correlation functions like Eq. (2.6). For an interval of scales where a variation of the Coulomb constant β is small, one can use for the function expression (2.17) where one should substitute the renormalized value of the Coulomb constant β. Analogously, the renormalized annihilation rate is determined by Eq. (3.3), where one should substitute expression (2.17) with the renormalized value of the Coulomb constant β. Next, for the renormalized creation rate we should use the relation

$$\overline{R}_{\tau_1} = \int d^2 r_0 \, S(\tau_1 - \tau_2, \boldsymbol{r}, \boldsymbol{r}_0) \overline{R}_{\tau_2}, \tag{3.13}$$

where $\tau_1 > \tau_2$. Relation (3.13) can be derived from Eq. (3.6) to use the property of S analogous to Eq. (3.1). For the renormalized creation rate, relation (3.13) is correct only if $\beta(r_1)$ weakly differs from $\beta(r_2)$ for characteristic values of the parameters $r_1 \sim \sqrt{\tau_1}$ and $r_2 \sim \sqrt{\tau_2}$.

A relation analogous to Eq. (3.13) can be formulated for the annihilation rate R. The relation leads to the same expression (3.3) where β is now scale dependent. Therefore the renormalized quantity of the annihilation constant λ_r flows together with β in accordance with Eq. (2.18). This accounts for the nonlogarithmic character of the integrals leading to relation (2.18).

Then we should define the renormalized fugacity in dynamics. For this purpose let us generalize expression (3.10)

$$\int_0^\infty d\tau \, \overline{R}_\tau(r) = \frac{y^2}{r^4}. \tag{3.14}$$

Then Eq. (3.10) is rewritten as

$$y = \left(\frac{a}{r}\right)^{\beta - 2} y_0. \tag{3.15}$$

The relation can be treated as an elementary step of the renormalization-group procedure, which is described by Eq. (1.5) for y. Thus the renormalization group equation for β in dynamics coincides with one in statics.

Expression (3.11) for the correction to the Coulomb constant β can be considered as arising at the elementary step of the renormalization-group procedure. The corresponding renormalization-group equation can be found to pass to the differential form and to substitute y_0 by the renormalized value y in accordance with Eq. (3.15). Then we obtain the renormalization-group equation coinciding with Eq. (1.5) for β. The expression (3.12) for the correction to the diffusion coefficient leads to the following renormalization-group equation:

$$\frac{dD}{d\ln(r/a)} \sim -y^2, \tag{3.16}$$

analogous to Eq. (1.5) for β. We conclude that the correction to D is small due to the small value of the fugacity and is therefore irrelevant. To avoid a misunderstanding, remember that the variation of the Coulomb constant β with increasing scale is also small. Nevertheless, as seen from Eq. (1.5), it is the difference $\beta - 2$ that enters the renormalization-group equations and the variation of the difference can be essential.

IV. CORRELATION FUNCTIONS

Here, we treat nonsimultaneous correlation functions of the charge density ρ, Eq. (1.2),

$$F_{2n}(t_1, \ldots, t_{2n}; \boldsymbol{r}_1, \ldots, \boldsymbol{r}_{2n}) = \langle \rho(t_1, \boldsymbol{r}_1) \ldots \rho(t_{2n}, \boldsymbol{r}_{2n}) \rangle. \tag{4.1}$$

Note an obvious consequence of the constraint (1.3)

$$\int d^2 r_1 \, F_{2n} = 0. \tag{4.2}$$

To examine the correlation functions (4.1) we use the representation (1.18). We will assume that all the diagrammatic blocks corresponding to small defect-antidefect pairs are already included in the renormalization of the corresponding coupling constants as discussed in Sec. III. Therefore, the fugacity y and the Coulomb constant β entering all subsequent expressions should be taken at the current scale. First we will examine contributions to the functions associated with a single defect-antidefect pair and then we will consider contributions related to a number of defect-antidefect pairs.

A. Pair correlation function

We start with the pair-correlation function

$$F_2(t_2 - t_1, \boldsymbol{r}_2 - \boldsymbol{r}_1) = \langle \rho(t_2, \boldsymbol{r}_2) \rho(t_1, \boldsymbol{r}_1) \rangle, \tag{4.3}$$

with $t_2 > t_1$. The average (4.3) can be calculated in accordance with relation (1.21) where one should substitute expression (1.18). We assume $t_f = t_2$.

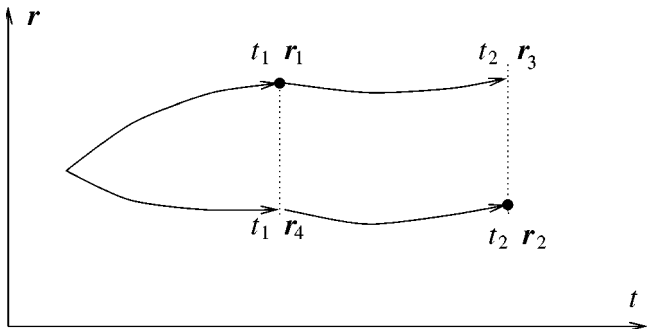

FIG. 9. Trajectories contributing to the pair-correlation function.

The contribution to the average (4.3) related to a single defect-antidefect pair can be represented by a series of the diagrams with two lines constituted of the defect and antidefect propagators. The lines start from the creation point. A half of the diagrams have the structure depicted in Fig. 9. Here we omitted lines and vertices corresponding to the interaction of the defects (which is implied) and keep only trajectories of the defects. The trajectories should pass through the points $\boldsymbol{r}_1$ and $\boldsymbol{r}_2$ at the time moments t_1 and t_2 (the events are designated by black circles). An additional contribution to the average (4.3) is determined by similar diagrams where both events $t_1,\boldsymbol{r}_1$ and $t_2,\boldsymbol{r}_2$ belong to the same trajectory.

As above, we dissect the diagram into parts that can be treated separately. Let us make a cut along planes in $\boldsymbol{r}-t$ space time corresponding to the time moments t_1 and t_2, they are shown in Fig. 9 by dotted lines. Intermediate points appearing in the convolution (3.1) are designated in Fig. 9 as $\boldsymbol{r}_3$ and $\boldsymbol{r}_4$. After that the diagram is divided into two parts separated by the dotted line. The part of the diagram to the right from the dotted line corresponds to the conditional probability M, Eq. (2.6), and the part of the diagram to the left from the dotted line corresponds to the correlation function

$$\Phi_2(\boldsymbol{r}_1-\boldsymbol{r}_2)=\langle \psi_+(t,\boldsymbol{r}_1)\psi_-(t,\boldsymbol{r}_2)\rangle. \tag{4.4}$$

The quantity (4.4) can be treated as the probability density to find a defect-antidefect pair with a given separation. Correspondingly, the integral $\int d^2r\,\Phi_2(\boldsymbol{r})$ determines the density of the defect-antidefect pairs. The correlation function (4.4) coincides with the integral on the left-hand side of Eq. (3.14). Hence

$$\Phi_2(r)=y^2/r^4, \tag{4.5}$$

where y is the renormalized fugacity. Equations (1.6) and (4.5) show that asymptotically in the low-temperature phase

$$\Phi_2(r)\propto r^{-2\beta}. \tag{4.6}$$

Note that the same behavior (4.6) is observed up to a slowly varying factor in the whole region of scales.

The diagram depicted in Fig. 9 gives a convolution of Φ_2 and M. Adding the contribution corresponding to the case where both events $t_1,\boldsymbol{r}_1$ and $t_2,\boldsymbol{r}_2$ belong to the same trajectory, we get the following expression for the pair-correlation function (4.3),

$$F_2(t,\boldsymbol{r}_2-\boldsymbol{r}_1)=-2\int d^2r_3\,d^2r_4\,\Phi_2(\boldsymbol{r}_4-\boldsymbol{r}_1)\times[M(t,\boldsymbol{r}_3,\boldsymbol{r}_2,\boldsymbol{r}_1,\boldsymbol{r}_4)-M(t,\boldsymbol{r}_2,\boldsymbol{r}_3,\boldsymbol{r}_1,\boldsymbol{r}_4)], \tag{4.7}$$

where $t>0$. At small times t we turn to the limit law (2.8). Substituting the expression into Eq. (4.7) we get

$$F_2(t=0,\boldsymbol{r}_1-\boldsymbol{r}_2)=2\,\delta(\boldsymbol{r}_1-\boldsymbol{r}_2)\int d^2r\,\Phi_2(\boldsymbol{r})-2\Phi_2(\boldsymbol{r}_1-\boldsymbol{r}_2). \tag{4.8}$$

Here the second contribution corresponds to the law (1.7) and the term proportional to the δ function is an autocorrelation contribution associated with a single defect. The factor in front of the δ function (which is the density of defects) is in accordance with the relation (4.2). Note that at small t the δ function is converted into a narrow function of the width $\sim\sqrt{t}$.

It follows from Eqs. (2.17), (4.5), and (4.7) that for $t\sim r^2$,

$$F_2(t,\boldsymbol{r})\sim\frac{y^2(r)}{r^4}. \tag{4.9}$$

To justify Eq. (4.9) one should check that there are no divergences in the integral (4.7). It can be done directly using Eq. (2.17). The convergence at small separations r and r_0 accounts for the behavior of the modified Bessel functions $I_\nu(x)\propto x^\nu$ at small values of the argument. The convergence at large separations r and r_0 can be checked using Eq. (2.9). If $|t|\gg r^2$ then

$$F_2\sim-\frac{y^2(r)}{r^{4-2\beta}|t|^\beta}. \tag{4.10}$$

The behavior of the pair-correlation function determined by the laws (4.9) and (4.10) corresponds to conventional critical dynamics (see, e.g., Ref. [24]) with the dynamical critical index $z=2$. However, as we will see below, the behavior of the high-order correlation functions is beyond the conventional scheme. Besides, the scaling law $t\sim r^2$ is true for the high-order correlation functions as well.

B. High-order correlation functions

Here we extend the procedure of the preceding subsection to the case of the high-order correlation functions F_{2n} (4.1). We will assume that $t_1<t_2<\ldots<t_{2n}$. Again, we examine the contribution to F_{2n} associated with a single defect-antidefect pair. Corresponding diagrams contain two trajectories starting anywhere and passing through the points $\boldsymbol{r}_1,\ldots,\boldsymbol{r}_{2n}$ at the time moments $t_1,\ldots,t_{2n}$. We will designate the trajectories of the defect and of the antidefect as $\boldsymbol{x}(t)$ and $\boldsymbol{z}(t)$.

Let us dissect the diagrams along planes in the $\boldsymbol{r}-t$ space time corresponding to the time moments $t_1,\ldots,t_{2n}$. Then the diagram is divided into a number of blocks, see Fig. 10. The left block in Fig. 10 corresponds to the object (4.4) and all the other blocks correspond to the correlation function

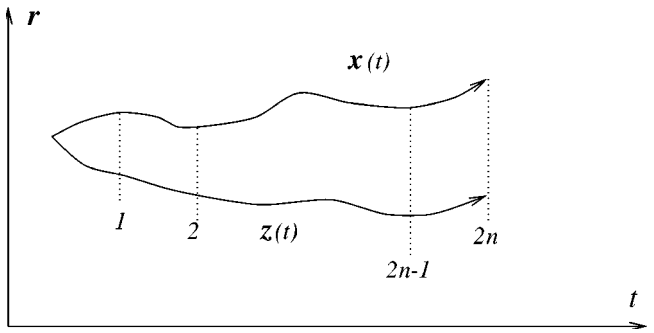

FIG. 10. Trajectories passing through a number of points.

(2.6). Again, using Eq. (3.1) we can write the contribution to the correlation function (4.1) associated with a single defect-antidefect pair as the following convolution:

$$F_{2n}(t_1,\ldots,t_{2n};\boldsymbol{r}_1,\ldots,\boldsymbol{r}_{2n}) = \prod_{j=1}^{2n} \int d^2x_j\, d^2z_j\, \Phi_2(\boldsymbol{x}_1-\boldsymbol{z}_1)[\,\delta(\boldsymbol{r}_j-\boldsymbol{x}_j) - \delta(\boldsymbol{r}_j-\boldsymbol{z}_j)]M(t_{j+1}-t_j,\boldsymbol{x}_{j+1},\boldsymbol{z}_{j+1},\boldsymbol{x}_j,\boldsymbol{z}_j). \quad (4.11)$$

Here, one must replace the last factor $M(t_{2n+1}-t_{2n})$ by unity. Relation (4.11) is a generalization of Eq. (4.7). Thus we got an expression for the correlation function that is a multiple integral of functions determined by explicit formulas.

An analysis shows that there are no divergences in the integrals at all steps of calculating F_{2n}. This means that we can evaluate the correlation functions from naive dimension estimates. Namely, if all space separations among $|\boldsymbol{r}_i-\boldsymbol{r}_j|$ are of the same order r_* and all time intervals are of the order r_*^2 then

$$F_{2n}\sim y^2(r_*)r_*^{-4n}. \quad (4.12)$$

In the large-scale limit when β is saturated, we have, in accordance with Eq. (1.6),

$$F_{2n}\propto r_*^{-4(n-1)-2\beta}. \quad (4.13)$$

If some space separations among $|\boldsymbol{r}_i-\boldsymbol{r}_j|$ and/or some time intervals differ strongly, then one can formulate some simple rules following from Eqs. (2.17) and (4.11). Let us give some examples. If one of the time intervals τ is much larger than all values of the squared separations $|\boldsymbol{r}_i-\boldsymbol{r}_j|^2$ then the correlation function behaves like $F_{2n}\propto\tau^{-\beta}$. For small τ, there appear contributions to F_{2n}, short correlated in space (on scales $\sim\sqrt{\tau}$). In the limit $\tau\to 0$ the contributions turn into δ functions, as it was for the pair-correlation function, see Eq. (4.8), representing an autocorrelation of single defects. If the points $\boldsymbol{r}_j$ can be divided into two ''clouds'' with a separation r between the clouds much larger than their sizes (and all time intervals are much smaller than r^2) then the principal r dependence of the correlation function F_{2n} is the same as in the function $\Phi_2(r)$, Eq. (4.5).

Remember that the charge density ρ is related to the curl of the gradient of the hexatic angle φ for hexatics and to the curl of the gradient of the order parameter phase for superfluid films. It is instructive to re-express our results in terms of the phase gradient circulations of $\nabla\varphi$ over a closed loop C:

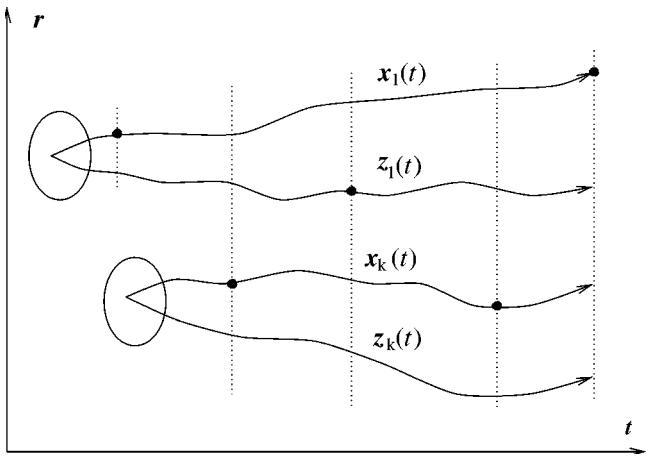

FIG. 11. A number of defect-antidefect pairs passing through given points.

$$\Gamma(t,C)=\oint d\boldsymbol{r}\,\nabla\varphi=2\pi\int d^2r\,\rho(t,\boldsymbol{r}), \quad (4.14)$$

where the second integral is taken over the area inside the loop. Correlation functions of Γ's can be rewritten as integrals of the correlation functions F_{2n}. As an example, consider the following average:

$$\Psi_{2n}=\langle\Gamma(t,C)\Gamma(t+\tau,C)\cdots\Gamma[t+(2n-1)\tau,C]\rangle. \quad (4.15)$$

Suppose that the characteristic size of the loop r is large enough so that we can assume that β is saturated, and that $\tau\sim r^2$. Then the following scaling law is satisfied: if $r\to Xr$ and $\tau\to X^2\tau$ then

$$\Psi_{2n}\to X^{4-2\beta}\Psi_{2n}, \quad (4.16)$$

where X is an arbitrary factor. The law (4.16) is a consequence of Eq. (4.13). It has two striking peculiarities. First, it possesses a clear critical dependence. Second, it is independent of the order n.

C. Many-pair contributions

We have established the contributions to the charge-density correlation functions F_{2n} associated with a single defect-antidefect pair. Now we are going to discuss other contributions to the correlation functions related to an arbitrary number of defect-antidefect pairs. Correspondingly, we should take diagrams with a number of trajectories passing through the points $\boldsymbol{r}_1,\ldots,\boldsymbol{r}_{2n}$ at the time moments $t_1,\ldots,t_{2n}$. The picture illustrating the situation is drawn in Fig. 11 where black circles correspond to the arguments of F_{2n}: $(t_1,\boldsymbol{r}_1),\ldots,(t_{2n},\boldsymbol{r}_{2n})$. There we omitted blocks related to short-living defect-antidefect pairs, regarding that the blocks are already included into the renormalization of the Coulomb constant β.

As previously, we can dissect the diagrams along the planes in the $\boldsymbol{r}-t$ space time corresponding to the time mo-

ments $t_1, \ldots, t_{2n}$. Then any diagram will be divided into a number of strips, see Fig. 11. The part of the diagram within each strip can be treated as the corresponding matrix element of the evolution operator $\exp(-\int dt\,\mathcal{H})$. Then the contribution to F_{2n} will be written like Eq. (4.11) as a convolution of the matrix elements. Generally, the matrix elements can be estimated like the function (2.6): each trajectory segment gives a factor that scales as $1/t$ and t scales as r^2. But there are obvious exceptions from the rule. Namely, going back in time we will come to a moment where a defect-antidefect pair was created. Again, when we consider small separations between the defect and the antidefect (which is correct for time moments close to the creation time) we can take into account only the Coulomb interaction between the two created defects. The corresponding regions in Fig. 11 are inside the ovals. Each such region produces the factor y^2. Therefore, generally $F_{2n} \propto y^{2k}$, where k is the number of the pairs. Taking into account also a scale-dependent factor we get

$$F_{2n} \sim y^{2k}(r_*) r_*^{-4n}, \tag{4.17}$$

where we assume that all space separations are of the order r_* and all time intervals are of the order r_*^2.

The expression (4.17) is a generalization of Eq. (4.12). Comparing these two expressions we see that the ratio of the contribution (4.17) to the contribution (4.12) is the $(k-1)$th power of a dimensionless small parameter $y^2(r_*)$. Thus we conclude that the leading contribution to F_{2n} is related to a single defect-antidefect pair, that corresponds to $k=1$. Now we can explain the origin of the estimate (1.8) for the simultaneous correlation functions, which obviously does not coincide with Eq. (4.12). The estimate (1.8) in terms of Eq. (4.17) corresponds to $k=n$. The reason is quite obvious: Two defects cannot pass simultaneously through $2n$ points and at least $k=n$ defect-antidefect pairs should be taken to obtain a nonzero contribution to the simultaneous correlation function F_{2n}. The situation is illustrated by Fig. 2. Note that the estimate (1.8) is not correct for the autocorrelation contributions proportional to δ functions, as written in Eq. (4.8).

Thus we have two different regimes: for simultaneous and for nonsimultaneous correlation functions. Let us establish the boundary between the regimes. For this purpose, we should consider small time intervals where the single-pair contribution is finite but small. The smallness is associated with diffusive exponents presented, e.g., in expression (2.17). Therefore the characteristic time where the simultaneous regime passes into the nonsimultaneous one can be estimated as

$$t \sim \frac{r^2}{|\ln[y(r)]|}, \tag{4.18}$$

where r is a space separation corresponding to the small time interval. In the low-temperature phase on large scales (where β is saturated) we have $|\ln y| \approx (\beta-2)\ln(r/a) + |\ln y 0|$.

V. SUPERFLUID FILMS

Let us consider superfluid films. The equation-of-motion for the vortices contains an additional term (Magnus force). Thus instead of Eq. (1.10) we should write (see Ref. [11])

$$\frac{dx_{j,\alpha}}{dt} = -\frac{D}{T}\left[\frac{\partial \mathcal{F}}{\partial x_{\alpha j}} + n_j \gamma \epsilon_{\alpha\beta} \frac{\partial \mathcal{F}}{\partial x_{\beta j}}\right] + \xi_{j,\alpha}, \tag{5.1}$$

where γ is a new dimensionless parameter. Equation (5.1) can be derived in the spirit of the procedure proposed by Hall and Vinen for the 3D superfluid, see Ref. [25]. Huber [26] argued that the same equation is correct for spin vortices in planar 2D magnetics.

For the superfluid films the ''charge density'' (1.2) is proportional to the vorticity $\operatorname{curl} \boldsymbol{v}_s$. To calculate correlation functions F_{2n}, Eq. (4.1), one can use the scheme developed in the previous sections. The only difference is that one should use the solution of the equation

$$\partial_t M = \left(\frac{1}{2}\nabla_\varrho^2 + 2\nabla_r^2 + 4\beta \frac{\boldsymbol{r}}{r^2}\nabla_r\right) M + 2\gamma\beta\epsilon_{\alpha\beta}\frac{r_\beta}{r^2}\nabla_{\varrho\alpha} M$$
$$- R(r) M + \delta(t)\,\delta(\boldsymbol{r}-\boldsymbol{r}_0)\,\delta\left(\varrho - \frac{\boldsymbol{r}_3}{2} - \frac{\boldsymbol{r}_4}{2}\right). \tag{5.2}$$

The variables $\boldsymbol{r}$, $\boldsymbol{r}_0$, and ϱ are introduced by Eq. (2.11). Again, on scales $r \gg a$ one can omit the term with the annihilation rate R in Eq. (5.2) demanding a finite value of M at $r \to 0$ instead.

Unfortunately, a cross term over $\boldsymbol{r}$ and ϱ appears in the operator on the right-hand side of Eq. (5.2). Thus one cannot obtain an explicit expression for M of the type of Eq. (2.9). Nevertheless, this additional term has the same dimensionality as the other terms and does not change the scaling estimates $M \sim t^{-2}$, $t \sim r^2$ determining the function M. Moreover, the equation for the object

$$S(t,\boldsymbol{r},\boldsymbol{r}_0) = \int d^2\varrho\, M(t,\boldsymbol{r},\varrho,\boldsymbol{r}_0,\boldsymbol{r}_3/2+\boldsymbol{r}_4/2), \tag{5.3}$$

following from Eq. (5.2) is identical to Eq. (2.13). Therefore, for the object (5.3), we have the same series (2.12) with the coefficients (2.17).

Looking through the derivation presented in Sec. III we see that just the function S (5.3) enters all the relations. Therefore, we can make the same assertions as previously. First, on large scales the annihilation coefficient λ is equal to its universal value (2.18). Second, we can write the same expression (4.5) for the average (4.4). Third, in dynamics we get the same renormalization-group equation (1.5) for β. Fourth, the renormalization of the diffusion coefficient is irrelevant. And finally, one can assert that a renormalization of the parameter γ introduced by Eq. (5.1) is determined by the equation

$$\frac{d\gamma}{d\ln(r/a)} \sim y^2,$$

analogous to Eq. (3.16). Therefore the renormalization of γ is irrelevant. Again, the scheme can be generalized to include the ''external potential,'' which now is the average value of the superfluid velocity.

Next, we proceed to the correlation functions F_{2n} (4.1). Formally they are determined by the same convolution (4.11) as previously. However, one should substitute there the solution of Eq. (5.2). Therefore the concrete expressions for F_{2n} will be different. Nevertheless, the estimates like Eqs. (4.12), (4.13), and (4.17) remain true because of the following reasons. First, due to the same dimensionality of all the terms on the right-hand side of Eq. (5.2), the function M possesses the simple scaling properties noted above. Second, there are no divergences in the convolutions such as Eq. (4.11) determining the objects. To prove the second property, we should analyze a behavior of M at large and at small separations. In the case $rr_0/t \gg 1$ the characteristic values of the separations $\boldsymbol{r}_1-\boldsymbol{r}_3$ and of $\boldsymbol{r}_2-\boldsymbol{r}_4$ are $\sim\sqrt{t}$ and are consequently much smaller than $|\boldsymbol{r}_1-\boldsymbol{r}_2|$ (or $|\boldsymbol{r}_3-\boldsymbol{r}_4|$). Then it is possible to neglect all the terms containing $|\boldsymbol{r}_1-\boldsymbol{r}_2|$ in denominators in Eq. (5.2) and we come to a purely diffusive equation leading to the corresponding asymptotics. It is possible to establish that the small scale of the conditional probability M for the vortices coincides with that examined above. The properties ensure convergence of all intermediate integrals appearing at calculating the correlation functions of vorticity F_{2n}.

We have also the same scaling law (4.16) for the correlation function (4.15) of the integrals (4.14) which are now proportional to the circulations of the superfluid velocity. We conclude that all the scaling laws for the correlation functions of the vorticity and their asymptotic behavior remains the same as previously.

VI. DISCUSSION

The main result of our consideration is the expression (4.12) for high-order correlation functions of the ''charge density'' (4.1) which is disclinicity for hexatic films and vorticity for superfluid films. We see from Eq. (4.12) that the high-order correlation functions are much larger than their normal estimates via the pair-correlation function. Namely, in accordance with Eqs. (4.9) and (4.12) we have

$$F_{2n}/F_2^n \sim y^{-2n+2} \gg 1, \tag{6.1}$$

where y is the renormalized fugacity. The asymptotic behavior of the ratio at large scales is determined by the law (1.6). Though at developing our scheme we accepted that the defect-antidefect pairs constitute a dilute solution, we hope that the scaling law (6.1) is universal. The ground for the hope is the renormalization-group procedure (formulated in Ref. [19]) which shows that on large scales we come to an effectively dilute solution of the pairs. We believe that the most interesting fact to be compared with experiment or numerics is the scaling law (4.16) which is a consequence of Eq. (6.1).

The physics behind the inequality (6.1) is as follows. The main contribution to the correlation functions is associated with a single defect-antidefect pair. Though the contribution associated with a number of defect-antidefect pairs contains an additional huge entropy factor it has also an additional small factor associated with small probability to observe defect-antidefect pairs with separations larger than the core radius a. The smallness is accounted for by the strong Coulomb attraction. The considered effect is a consequence of the competition of those two factors. The result of the competition manifests in the law (4.17) which gives the estimate for the contribution associated with k defect-antidefect pairs. For simultaneous correlation functions nothing similar occurs and we have the conventional estimate (1.8). That is the reason why the effect cannot be observed in statics. The property is directly related to causality since a defect-antidefect pair cannot simultaneously pass through $2n$ points and at least n defect-antidefect pairs are needed to get a nonzero contribution to the simultaneous correlation function F_{2n}, see Fig. 2. That explains the estimate (1.8). Thus we have two different regimes for simultaneous and nonsimultaneous correlation functions. The characteristic boundary time separating those two regimes is written in Eq. (4.18).

The considered effect resembles intermittency in turbulence (see, e.g., Ref. [14]) leading to large r-dependent factors in the ratios like in Eq. (6.1) in the velocity correlation functions of a turbulent flow. However, as is seen from Eq. (6.1), for the defects, the large r-dependent factors are related to the ultraviolet cutoff parameter a whereas for intermittency in turbulence the large r-dependent factors are related to the infrared (pumping) scale. Our situation is thus closer to the inverse cascade (see Ref. [27]) realized on scales much larger than the pumping length. There are experimental data [28] concerning the inverse cascade in 2D hydrodynamics and analytical observations concerning the inverse cascade for a compressible fluid [29] that indicate the absence of the intermittency in the inverse cascades. Note that only simultaneous objects were examined in the papers in Refs. [28] and [29], and there is no intermittency in our simultaneous correlation functions. So, based on the analogy, one may think that for the inverse cascades, nonsimultaneous objects reveal some intermittency.

The consideration presented in our paper is applicable to superfluid films. There exist also films and quasi-2D systems of different symmetry. Huber [26] argued that the same equation as for quantum vortices is correct for spin vortices in planar 2D magnets. We believe that our approach, based on Eq. (1.10), is correct for the dynamics of disclinations in hexatic films such as membranes, freely suspended films, and Langmuir films. Next, the above scheme seems to work also for dislocations in solid films. The system needs a special treatment since a modification should be introduced into the procedure. Maybe some features of the presented picture can be observed also in superconductive materials, especially in high-T_c superconductors. There are analytical and numerical indications that for purely Langevin dynamics of the order parameter, there are logarithmic corrections to the law (1.10), see Refs. [30–36].

ACKNOWLEDGMENTS

I am grateful to G. Falkovich, K. Gawedzki, I. Kolokolov, and M. Vergassola for useful discussions and to E. Balkovsky, A. Kashuba, and S. Korshunov for valuable remarks. This research was supported in part by a grant from the Israel Science Foundation, by a grant from the Minerva Foundation, and by the Landau-Weizmann Prize program.

[1] V. L. Berezinskii, Zh. Éksp. Teor. Fiz. **59**, 907 (1970) [Sov. Phys. JETP **32**, 493 (1971)]; Zh. Éksp. Teor. Fiz. **61**, 1144 (1971) [Sov. Phys. JETP **34**, 610 (1972)].
[2] J. M. Kosterlitz and D. J. Thouless, J. Phys. C **5**, L124 (1972); **6**, 1181 (1973).
[3] J. M. Kosterlitz and D. J. Thouless, in *Progress in Low Temperature Physics*, edited by D. F. Brewer (North-Holland, Amsterdam, 1978), Vol. VII B, p. 373.
[4] D. R. Nelson, in *Fundamental Problems in Statistical Mechanics*, edited by E. G. D. Cohen (North-Holland, Amsterdam, 1980), Vol. V, p. 53.
[5] D. R. Nelson, in *Phase Transitions and Critical Phenomena*, edited by C. Domb and J. L. Lebowitz (Academic, London, 1983), Vol. 7, p. 1.
[6] P. Minnhagen, Rev. Mod. Phys. **59**, 1001 (1987).
[7] Z. Gulacsi and M. Gulacsi, Adv. Phys. **47**, 1 (1998).
[8] D. R. Nelson and J. M. Kosterlitz, Phys. Rev. Lett. **39**, 1201 (1977); B. I. Halperin and D. R. Nelson, *ibid.* **41**, 121 (1978); **41**, 519 (1978); A. P. Young, Phys. Rev. B **19**, 1855 (1979); D. R. Nelson and B. I. Halperin, *ibid.* **19**, 2457 (1979).
[9] K. J. Strandburg, Rev. Mod. Phys. **60**, 161 (1988).
[10] G. Blatter, M. V. Feigel'man, V. B. Geshkenbein, A. I. Larkin, and V. M. Vinokur, Rev. Mod. Phys. **66**, 1125 (1994).
[11] A. Ambegaokar, B. I. Halperin, D. R. Nelson, and E. D. Siggia, Phys. Rev. Lett. **40**, 783 (1978); Phys. Rev. B **21**, 1806 (1980).
[12] A. Zippelius, B. I. Halperin, and D. R. Nelson, Phys. Rev. B **22**, 2514 (1980); R. Bruinsma, B. I. Halperin, and A. Zippelius, *ibid.* **25**, 579 (1982).
[13] M. Doi, J. Phys. A **9**, 1465,1479 (1976).
[14] U. Frisch, *Turbulence: The Legacy of A. N. Kolmogorov* (Cambridge University Press, New York, 1995).
[15] I. Lifshits, S. Gredeskul, and A. Pastur, *Introduction to the Theory of Disordered Systems* (Wiley Interscience, New York, 1988).
[16] K. B. Efetov, *Supersymmetry in Disorder and Chaos* (Cambridge University Press, Cambridge, 1997).
[17] V. V. Lebedev, Pis'ma Zh. Éksp. Teor. Fiz. **70**, 675 (1999) [JETP Lett. **70**, 691 (1999)].
[18] V. V. Lebedev, e-print cond-mat/9904430.
[19] J. M. Kosterlitz, J. Phys. C **7**, 1046 (1974).
[20] J. V. Jose, L. P. Kadanoff, S. Kirkpatrick, and D. R. Nelson, Phys. Rev. B **16**, 1217 (1977).
[21] L. P. Kadanoff, Ann. Phys. **120**, 39 (1979); L. P. Kadanoff and A. B. Zisook, Nucl. Phys. B **180**, 61 (1981).
[22] L. Peliti, J. Phys. (Paris) **46**, 1469 (1985).
[23] L. Peliti, J. Phys. A **19**, L365 (1986).
[24] P. C. Hohenberg and B. I. Halperin, Rev. Mod. Phys. **49**, 435 (1977).
[25] H. E. Hall and W. F. Vinen, Proc. R. Soc. London, Ser. A **238**, 215 (1956); W. F. Vinen, in Progress in *Low Temperature Physics* (North-Holland, Amsterdam, 1961), Vol. III, p. 1; P. Nozieres and W. F. Vinen, Philos. Mag. **14**, 667 (1966).
[26] D. L. Huber, Phys. Rev. B **26**, 3758 (1982).
[27] R. Kraichnan, Phys. Fluids **10**, 1417 (1967); J. Fluid Mech. **47**, 525 (1971).
[28] J. Paret and P. Tabeling, Phys. Fluids **10**, 3126 (1998).
[29] M. Chertkov, I. Kolokolov, and M. Vergassola, Phys. Rev. Lett. **80**, 512 (1998); M. Chertkov, I. Kolokolov, and M. Vergassola, Phys. Rev. E **56**, 5483 (1997); K. Gawedzki and M. Vergassola, e-print cond-mat/9811399.
[30] P. E. Chadis, W. van Saarloos, P. L. Finn, and A. R. Kortan, Phys. Rev. Lett. **58**, 222 (1987).
[31] H. Pleiner, Phys. Rev. A **37**, 3986 (1988).
[32] A. Pargellis, N. Turok, and B. Yurke, Phys. Rev. Lett. **67**, 1570 (1991).
[33] G. Ryskin and M. Kremenetsky, Phys. Rev. Lett. **67**, 1574 (1991).
[34] C. D. Muzny and N. A. Clark, Phys. Rev. Lett. **68**, 804 (1992).
[35] B. Yurke, A. N. Pargellis, T. Kovacs, and D. A. Huse, Phys. Rev. E **47**, 1525 (1993).
[36] S. E. Korshunov, Phys. Rev. B **50**, 13616 (1994).